Efficient control of quantum paths via dual-gas high harmonic generation

2011 New J. Phys. 13 113001

(http://iopscience.iop.org/1367-2630/13/11/113001)

New Journal of Physics
The open-access journal for physics

Efficient control of quantum paths via dual-gas high harmonic generation

A Willner[1,2,9], F Tavella[2], M Yeung[3], T Dzelzainis[3], C Kamperidis[4], M Bakarezos[4], D Adams[3], R Riedel[2,7], M Schulz[1,7], M C Hoffmann[8], W Hu[8], J Rossbach[7], M Drescher[7], V S Yakovlev[5,6], N A Papadogiannis[4], M Tatarakis[4], B Dromey[3] and M Zepf[3]

[1] Deutsches Elektronen Synchrotron, Notkestrasse 85, 22607 Hamburg, Germany
[2] Helmholtz-Institute Jena, Max-Wien-Platz 1, 07743 Jena, Germany
[3] Queens University, University Road, Belfast BT7 1NN, UK
[4] Centre for Plasma Physics and Lasers, TEI of Crete, E Daskalaki 1 Str., 74100 Rethymno and Romanou 3 Str., 73133 Chania, Crete, Greece
[5] Max-Planck-Institute of Quantum Optics, Hans-Kopfermann-Str. 1, 85748 Garching, Germany
[6] Department für Physik, Ludwig-Maximilians-Universität, Am Coulombwall 1, D-85748 Garching, Germany
[7] University of Hamburg, Luruper Chaussee 149, 22603 Hamburg, Germany
[8] Max Planck Research Department for Structural Dynamics, University of Hamburg, CFEL, Notkestrasse 85, 22607 Hamburg, Germany
E-mail: arik.willner@desy.de

New Journal of Physics **13** (2011) 113001 (14pp)
Received 31 July 2011
Published 3 November 2011
Online at http://www.njp.org/
doi:10.1088/1367-2630/13/11/113001

Abstract. The accurate control of the relative phase of multiple distinct sources of radiation produced by high harmonic generation is of central importance in the continued development of coherent extreme UV (XUV) and attosecond sources. Here, we present a novel approach which allows extremely accurate phase control between multiple sources of high harmonic radiation generated within the Rayleigh range of a single-femtosecond laser pulse using a dual-gas, multi-jet array. Fully ionized hydrogen acts as a purely passive medium and allows highly accurate control of the relative phase between each harmonic

[9] Author to whom any correspondence should be addressed.

source. Consequently, this method allows quantum path selection and rapid signal growth via the full coherent superposition of multiple HHG sources (the so-called quasi-phase-matching). Numerical simulations elucidate the complex interplay between the distinct quantum paths observed in our proof-of-principle experiments.

Contents

1. Introduction

The generation of coherent extreme UV (XUV) pulses of attosecond-to-femtosecond duration via the nonlinear process of high harmonic generation (HHG) [1, 2] is of substantial interest for applications in ultrafast science [3–6] and the external seeding of free electron lasers (FELs) [7]. However, the applicability of such XUV sources suffers from the low photon flux and, under certain circumstances, limited temporal and spatial coherence. Achieving both full coherent control and a higher conversion efficiency needs to be the focus of any new generation concept of high-order harmonic generation.

Unlike harmonic generation in conventional nonlinear optical processes (such as frequency doubling of lasers in nonlinear crystals), where the phase of the laser is directly related to that of the harmonic beam, HHG does not result in a unique phase relationship between a harmonic photon and the driving laser at the single atom level. The underlying physical mechanism is easily understood using the three-step model [8], whereby the electron first gets ionized via tunnel ionization, is subsequently accelerated in the laser field and finally releases the kinetic and ionization energy in the form of a harmonic photon. Since tunnel ionization is a continuous process during each laser cycle, there are a number of quantum paths that any given electron can take. Specifically, there are two paths that result in a recollision with the parent ion during the first laser cycle *and* with the same kinetic energy—the so-called long and the short trajectories [9]. As the names suggest, they are differentiated by the amount of time the electron takes between ionization and recollision and this is shown schematically in figure 1. The long trajectory corresponds to electrons released just beyond the peak of the laser electric field, while the short trajectory corresponds to electrons with the same return energy released just before the first zero-crossing of the field. Expressed in terms of the laser period T the short (long) trajectory correspond to durations of $\tau < 0.65\mathrm{T}$ ($\tau > 0.65\mathrm{T}$) between ionization and recollision with parent ion [10]. The path-dependent phase difference between the fundamental and harmonic radiation is given by the quasi-classical action of the electron [9] and is thus linearly dependent on the intensity of the driving laser such that $\phi^j_{\mathrm{QP}} = \alpha^j_q I$. The proportionality constant α^j_q is approximately proportional to the travel time τ^j_q for the qth-order harmonic (where j indicates the specific quantum path). These competing quantum paths are of

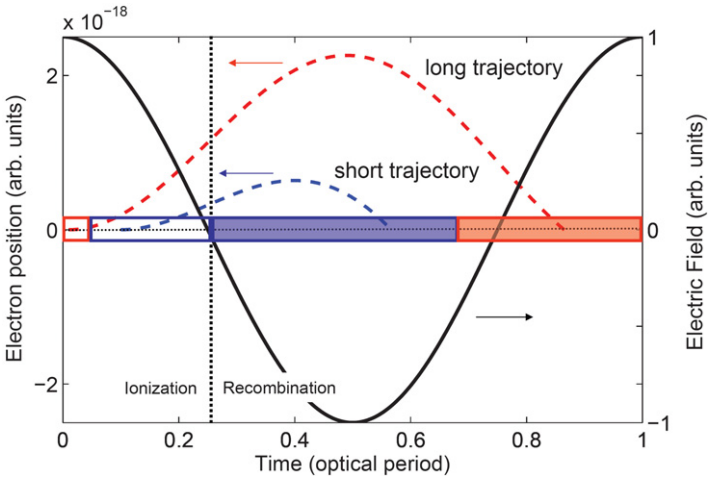

Figure 1. Concept of two electron trajectories in HHG. Ionization and recombination times for the long (red area) and short (blue area) trajectory in a driving laser field (black solid). Two example trajectories are implemented for a short trajectory (dashed blue) ionized at $T = 0.1$ and a long trajectory (dashed red) ionized at $T = 0.01$. They are plotted as electron position with respect to the parent ion versus time.

approximately equal strength and have a strong influence on the temporal and spatial coherence properties [11]. For example, due to the weaker intensity dependence of the quantum-path phase ϕ^j_{QP}, the phase front curvature of the short trajectory contribution is smaller than that for the long trajectory contribution, leading to a reduced divergence and to a higher degree of spatial coherence [12]. Secondly, the strong laser intensity variation from cycle to cycle typical of HHG experiments results in different return times for electrons with a given kinetic energy and hence the intensity-dependent phase degrades the periodicity of the HHG process, resulting in a complex spectral structure. Again this effect is much more pronounced for the long trajectory. Therefore achieving the highest coherence of the harmonic beam is best achieved by the selection of a short quantum path. One possible method leading to a high degree of coherence is to select only harmonics near the harmonic cut-off corresponding to a trajectory length of 0.65 T, where the two quantum paths become degenerate. The significantly reduced efficiency at high harmonic orders near the cut-off makes this approach undesirable from the perspective of achieving efficient harmonic generation, although it provides a convenient route for generating isolated attosecond pulses [13].

Another approach is to exploit the distinct intensity dependence of the return phase of the two quantum paths in combination with the phase-matching conditions in the generating medium. Coherent build-up of the harmonic signal throughout requires that the nonlinear medium is shorter than one coherence length $L_{\mathrm{c}} = \pi/\Delta k$, i.e. that the radiation generated at the beginning of the medium should be less than half a wave out of phase with radiation generated at the end of the medium. Clearly, any changes in laser intensity along the propagation path will affect the phase of the quantum path contribution and add a phase mismatch Δk^j_{QP} due to the intrinsic physics of the HHG process. The total phase mismatch is then given by the sum of atomic phase for each quantum path and the phase mismatch due to propagation in the medium $\Delta k = \Delta k^j_{\mathrm{QP}} + \Delta k_{\mathrm{prop}}$, whereby the propagation phase is typically dominated by the

plasma dispersion due to free electrons in the limit of strong ionization. Controlling the focusing, medium density and laser intensity it is therefore possible to approximately compensate for the phase mismatch of the desired quantum path and therefore achieve significantly different coherence lengths for the two trajectories, which allows a degree of quantum path control [14, 15].

Achieving full coherent control of the contributions of the two quantum paths and hence optimal coherence properties requires extremely accurate control of the phase-matching conditions in the medium. An attractive concept for achieving such a level of control is to separate the harmonic generation process from phase matching by coherently adding multiple harmonic generation zones created by the same laser—an approach known as quasi-phase-matching (QPM) [16]. In the case of HHG, QPM is typically implemented by allowing the signal to build up over one coherence length (the HHG half-period) and subsequently suppressing HHG for another coherence length (the matching half-period) until the driving field and harmonic field are in phase again. Perfect phase control between separate HHG sources therefore allows one quantum path to be selected. Since the intensity of N atoms emitting radiation coherently increases as N^2 under phase-matched conditions QPM also enables an $(N_{\mathrm{QPM}})^2$ increase in total pulse energy through coherent superposition of N_{QPM} individual sources [17]. In this paper, we present the concept of a novel dual-gas QPM approach which allows the phase between two HHG sources to be controlled with the extreme accuracy required for generating well-defined attosecond pulses [18, 19] and the coherent control of the pulse properties critical for FEL seeding [14, 20].

2. Dual-gas quasi-phase-matching

QPM can be achieved by any means that allows one to modulate the strength of the source term: for example, by varying the driving laser intensity with modulated capillary diameters [16, 21] or multi-mode beating in a capillary [22, 23], by using counterpropagating pulses [24] and by polarization gating [25]. Alternatively, the atomic density of the generation medium can be modulated [15, 26] either using multiple jets [17, 27] or by a capillary discharge [28]. These approaches have been highly effective in demonstrating the validity of the QPM principle to HHG, but still leave room for improvement in terms of coherent control of the quantum paths and achieving signal growth close to the ideal $(N_{\mathrm{QPM}})^2$ scaling.

An ideal QPM scheme should allow the HHG yield of the source to be limited only by absolute constraints of the medium itself (such as the absorption length and harmonic polarizability of a single atom or ion χ_q). To achieve this, the matching half-period should be completely passive (no HHG signal produced) and allow full and easily tuneable control of the phase between individual sources. This allows clean trajectory selection and rapid growth of the HHG signal to be achieved. Secondly, the matching half-period should negligibly absorb both harmonic and laser fields. Furthermore, since the high intensities required for HHG can only be achieved in the Rayleigh length of a laser beam, it is desirable to have the QPM periods as closely spaced as possible, thus maximizing the number of QPM periods within the Rayleigh range. The effects of absorption and imperfect suppression for QPM schemes that have ideal periodicity of $2L_{\mathrm{c}}$ are shown in figure 2. Note that reduction in the signal growth due to non-ideal modulation depth and absorption can be very substantial. Additionally, high-peak-power [29] or high-average-power applications using present-day lasers [30, 31] require a generation setup free of damage threshold constraints such as under circumstances where

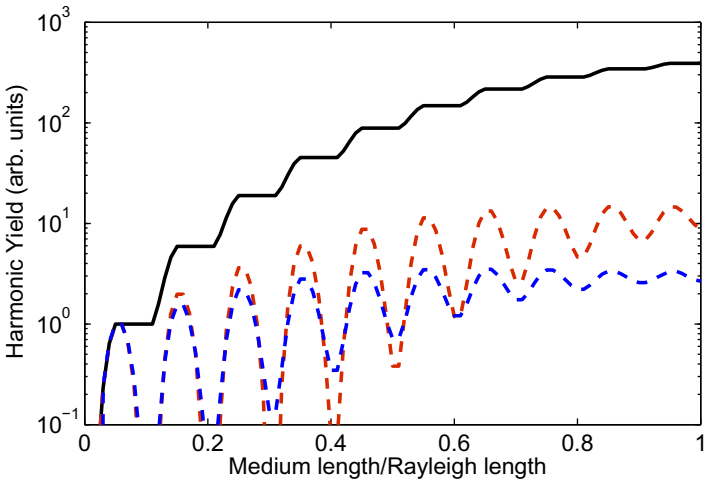

Figure 2. Signal growth for different QPM scenarios. Harmonic yield with $N_{\mathrm{QPM}} = 10$ in the focus of a Gaussian beam. Phase matching is assumed to be ideal for all cases and the medium extends over one Rayleigh range centered at the focus. Ideal QPM (no absorption and full modulation depth, black line) results in rapid signal growth. For comparison, QPM with a sinusoidal intensity modulation of 4% is shown without absorption (dashed red line) and with absorption assuming a medium with a length of two absorption lengths (dashed blue line).

the wall load is very high—such as multi-mode capillaries [23]—or when high-average-power systems are used being of particular interest for FEL seeding due to FEL pulse repetition rates of up to 1 MHz [20].

All the QPM schemes presented above, while elegant advances in their own right (in particular the use of counterpropagating pulses [24]), fall short of the ideal scenario discussed here, either because the source in the matching half-period is only weakly suppressed, the gas in the matching half-period adds appreciable absorption and/or because the spacing of multiple jets requires distances longer than common Rayleigh lengths. Among the basic concepts discussed above, free-propagating geometries appear to be the only solution meeting the requirements of high average power applications and therefore free jets appear to be best suited for generating the target setup.

Multi-jet arrays have been theoretically investigated [32, 33] and first experiments have been performed using the Gouy phase shift as the matching parameter in vacuum intersections between multiple sources [17, 27]. The one-dimensional (1D) theory predicts remarkable control of the relative weight of quantum path contributions on-axis and the possibility of substantial signal gain. In practice, the ionization-induced defocusing not included in the original theory complicates the evolution of the relative phase from the idealized vacuum Guoy shift and results in a jet separation which is substantial compared to the Rayleigh range of the laser. This implies that it is not possible to utilize the large number of jets required for high-quality coherent control or substantial signal gain.

In order to meet all requirements stated above, we developed a novel QPM multi-jet concept in which a generation medium alters with hydrogen as a passive matching medium (see figures 3(a) and (b)). The only restriction within dual-gas QPM is that the HHG medium

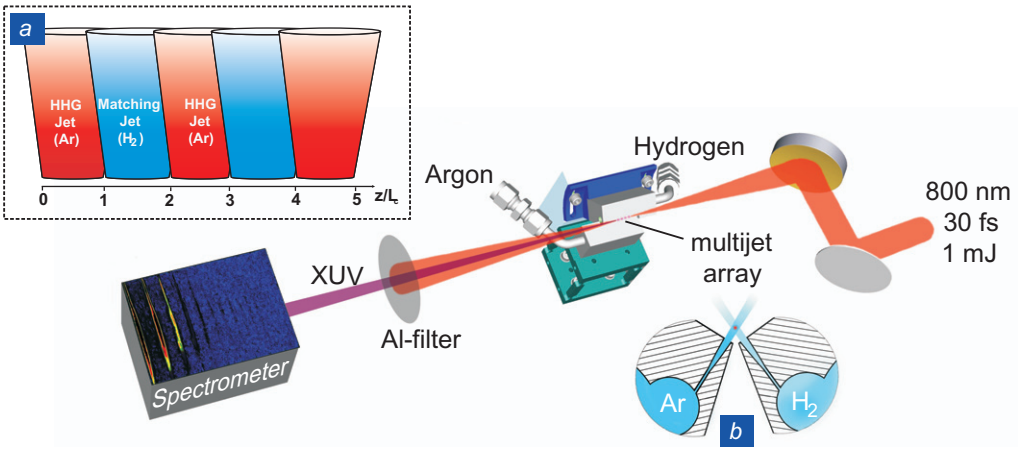

Figure 3. Experimental setup and principle. A gas-jet array consisting of two or more argon HHG jets interspersed with hydrogen phase-matching jets allows full control of the relative phase between the source jets by varying the hydrogen pressure. The jet array was irradiated with 30 fs pulses with an energy of 1 mJ from a Ti:sapphire laser system (800 nm) with a peak intensity in vacuum of 8×10^{14} W cm^{-2}. The fundamental laser light is filtered by two 200 nm Al filters and the XUV pulses are detected by an angularly resolving flatfield spectrometer. Due to geometrical constraints, the highest observable order was 41. Inset (a) shows a schematic diagram of the jet array with argon HHG jets alternating with hydrogen-matching jets with a periodicity of $2L_c$. (b) Cross-section of the prototype target with crossing jets.

must have a significantly higher ionization potential than atomic hydrogen (e.g. most of the common HHG media such as helium, neon, argon and their ions). If this condition is fulfilled, hydrogen will be fully ionized at the rising edge of the pulse. Since completely ionized hydrogen cannot emit further harmonic photons, the first condition for an ideal QPM scheme is perfectly met. Neutral and depleted hydrogen have minimal absorption for all wavelengths of interest compared to HHG media available and therefore the hydrogen half-period also fulfills the second condition and only adds a phase dominated by the free-electron dispersion such that

$$\phi_q \propto q L_M n_e r_e \lambda, \tag{1}$$

where L_M is the length of the matching half-period, n_e the electron density, r_e the classical electron radius and λ the fundamental wavelength.

The jet design used as a dual-gas multi-jet array is shown in figure 4(a). The jets are formed by electro-eroded Laval-shaped nozzles with a diameter of 200 μm at the nozzle exit. The separation of the nozzle centers is 430 μm center-to-center. The Laval shape is important for reducing the spread of the gas after exiting the nozzle and therefore serves to minimize turbulence between neighboring jets. The nozzle support is constructed in a way that the arrays of argon and hydrogen have a crossing angle of 15°, which leads to a crossing distance to the two nozzle entrances of about 150 μm. The argon array is placed on a solid spring for fine adjustment of the relative position of the two jet assemblies. The distance between the driver and the matching jet is as small as 230 μm center-to-center. The backing pressures in the two arrays

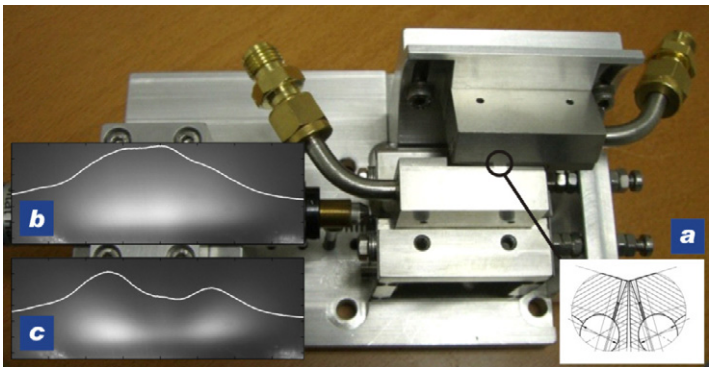

Figure 4. The proof-of-principle target. (a) Picture and working principle of the target used at TEI Crete. (b) Plasma side image for just argon and (c) for argon with one hydrogen intersection.

are controlled separately with absolute electronic pressure controllers, whereas all nozzles of the same array are operated with the same backing pressure. Arrays with either two HHG jets and one matching jet or four HHG jets interspersed with three matching jets are part of the proof-of-principle design.

Hydrogen as a matching medium within dual-gas QPM does not only add a phase difference between the laser and XUV fields. It also acts as a spacer between the sources, which ensures a high modulation amplitude, leading to sharp edges of generation and matching zones. Figures 4(b) and (c) show plasma side images of an array with two generation zones and one matching zone. In figure 4(b), no hydrogen is used so that the generation jets (e.g. argon in this case) fill the complete interaction area. By adding the hydrogen (figure 4(c)) two distinct generation jets become visible with the weakly emitting hydrogen plasma in the center.

In conclusion, the novel dual-gas QPM scheme combines the theoretical advantages of QPM for achieving high signal levels with a free propagating geometry that is suitable for converting high-power lasers. Dual-gas QPM is, in principle, compatible with producing bright harmonic spectra at short wavelengths approaching the *water window* and beyond. Phase-matched operation at such short wavelengths has recently been demonstrated by Popmintchev *et al* [34] using very long laser wavelengths where phase matching is easier to achieve at the cost of substantially reduced single-atom response ($\propto \lambda_L^{-6}$). Compared to this approach, dual-gas QPM operation has the added flexibility of being largely independent of driver wavelength and medium and may thus allow the strong harmonic response using high-power, shorter-wavelength drive lasers to be harnessed. To achieve ideal performance the phase introduced by each matching half-period would have to be varied freely from one hydrogen zone to the next. This is important because it is very difficult to achieve perfectly uniform conditions over long lengths along a high-power laser focus and especially for very high orders (e.g. sub-10 nm wavelengths) the laser field will experience sub-cycle modifications due to non-adiabatic effects in the generation medium [32]. This implies that L_c is not a constant along the propagation path and the dual-gas QPM scheme should allow for fine-tuneability to ensure that the total phase added by each QPM period corresponds to 2π. This feature, being in principle possible, will be implemented in future versions of the dual-gas multi-jet array allowing more than ten generation jets in the sub-10 nm regime. This will, of course, put high demands on the vacuum pumping

system, because in contrast to capillary-based HHG, higher backing pressures are needed in a free-jet system for achieving adequate signal in the short-wavelength regime.

However, for all wavelengths of interest it needs to be ensured that the absorption length of the systems is larger than the total length of the generation medium within the dual-gas array. Only if this condition is fulfilled, the QPM effect will lead to effective control of the quantum path contributions.

3. Quantum path control

The effectiveness of the dual-gas approach of achieving signal enhancements via QPM is the subject of a separate publication [35], in which we highlight the achievement of the full theoretical enhancement (36×) for an array consisting of six QPM periods.

The ability to coherently tune the relative weight of short and long trajectory contributions with dual-gas QPM was tested in the simplest geometry consisting of two argon jets for the HHG half-periods and one hydrogen jet for the matching half-period irradiated with 30 fs pulses from a titanium–sapphire laser with pulse energies of 1 mJ and at a repetition rate of 1 kHz (see figure 3). The central wavelength was 800 nm. The laser was focused with a parabolic mirror and a focal length of $f = 15$ cm into the gas array leading to a peak intensity up to 8×10^{14} W cm^{-2} with a focal spot size of 40 μm (full-width at half maximum, FWHM). The XUV radiation was detected using a flatfield XUV spectrometer coupled to an ANDOR CCD (type 435-BN, 13×13 μm pixel size), which resulted in an angular field-of-view of approximately 15 mrad. The Hitachi flatfield grating was calibrated at the Daresbury Synchrotron source to be able to extract absolute efficiencies from the measurement. The gas array was positioned 1 mm before the focal spot in order to increase the effect of the intrinsic phase [15]. In addition, the harmonics investigated were chosen to be well within the plateau region of the spectrum to ensure that long and short trajectory tuning is well distinguishable. Figure 5(a) shows the effect of varying the hydrogen pressure between the two argon generation jets. The 2 bar backing pressure for the argon jets has been chosen such that the N^2 increase in the angularly and spectrally integrated harmonic yield has stopped for all wavelengths visible in the spectrum. In addition, the absorption length for the 27th (41st) harmonic is about 20 mm (11 mm) for 14 torr in argon and thus much longer than the total generation zone (14 torr has been determined to be the actual argon pressure at 2 bar backing pressure using interferometric techniques [36]). Hence, it becomes obvious that pure phase tuning takes place by varying the hydrogen pressure.

To fully understand the physics behind these data, we look at the 41st and 27th harmonics in more detail. Figure 5(b) shows an oscillation of the harmonic yield of the 41st harmonic with two peaks at 1 bar and around 2.5 bar hydrogen pressure. The spectrally integrated lineout reveals an asymmetric shape of the oscillation. Since changing the density of the fully ionized hydrogen only affects the relative phase between the two sources, such behavior would not be expected for a well-defined relationship between laser and harmonic phase (i.e. where only one trajectory was present). Under such circumstances a periodic oscillation with hydrogen pressure should be observed. The asymmetry in the oscillation becomes even more obvious in figure 5(c) where the 27th harmonic is tuned with hydrogen. We can see a spectral splitting in the color plot and the two spectral components seem to be tuned separately by hydrogen. The spectrally integrated linout shows an asymmetry which originates in the superposition of the two spectral features. By separating the two components (red and black curves in the lineout plot) a smooth oscillation can be observed for each of them.

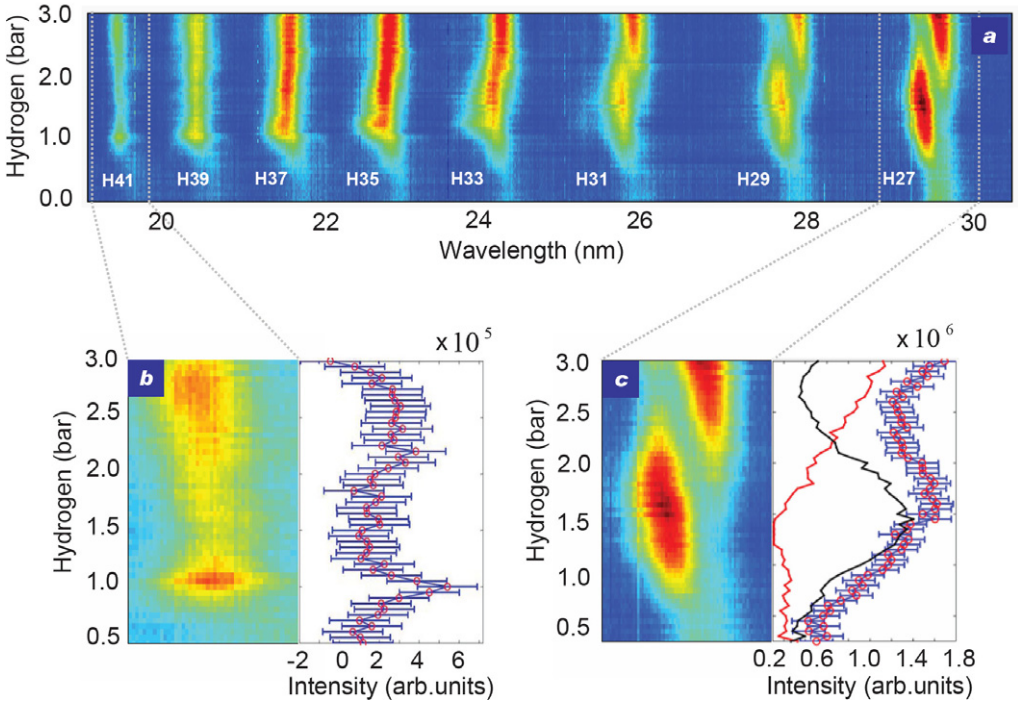

Figure 5. Results for the two-source array. Coherent superposition of two HHG jets with a 2 bar argon pressure and varying hydrogen backing pressure in the matching jet. (a) Hydrogen pressure scan from the 27th to the 41st harmonic. (b) Enlarged view of the hydrogen scan for the 41st harmonic and (c) for the 27th harmonic. Lineouts show the spectrally integrated harmonic yield (red dots) and for the 27th in addition the contribution of the shorter (black line) and longer wavelength components (red line). The oscillation of the harmonic yield with hydrogen pressure is clearly visible. The error bars indicate the error due to background subtraction.

This behavior can be understood in terms of the two distinct quantum trajectories. As discussed in section 1, these trajectories correspond to different ionization and recollision times, but should have the same electron kinetic energy upon return to the atom and consequently result in the emission of photons with approximately the same frequency. However, because of the effects of intercycle ionization and variation in the laser intensity, the exact emission frequency can be slightly different for the two quantum paths resulting in spectral splitting of each harmonic, which is clearly visible for the 27th harmonic in figure 5.

To distinguish the effects of the different trajectories from other effects on the harmonic spectral shape [37], we performed 3D simulations considering each trajectory separately. The simulation was performed with a 3D code based on the saddle-point analysis of the Lewenstein model for the single-atom dipole response [38, 39] allowing the inclusion of arbitrary quasi-static ionization rates and atom-specific recombination matrix elements. In addition, it provides a tool to study the contributions of the long and short trajectories separately, which is important for our purpose. The detailed theoretical model behind the simulation is described in several publications [40–42]. The code was modified to simulate a multi-jet array with hydrogen

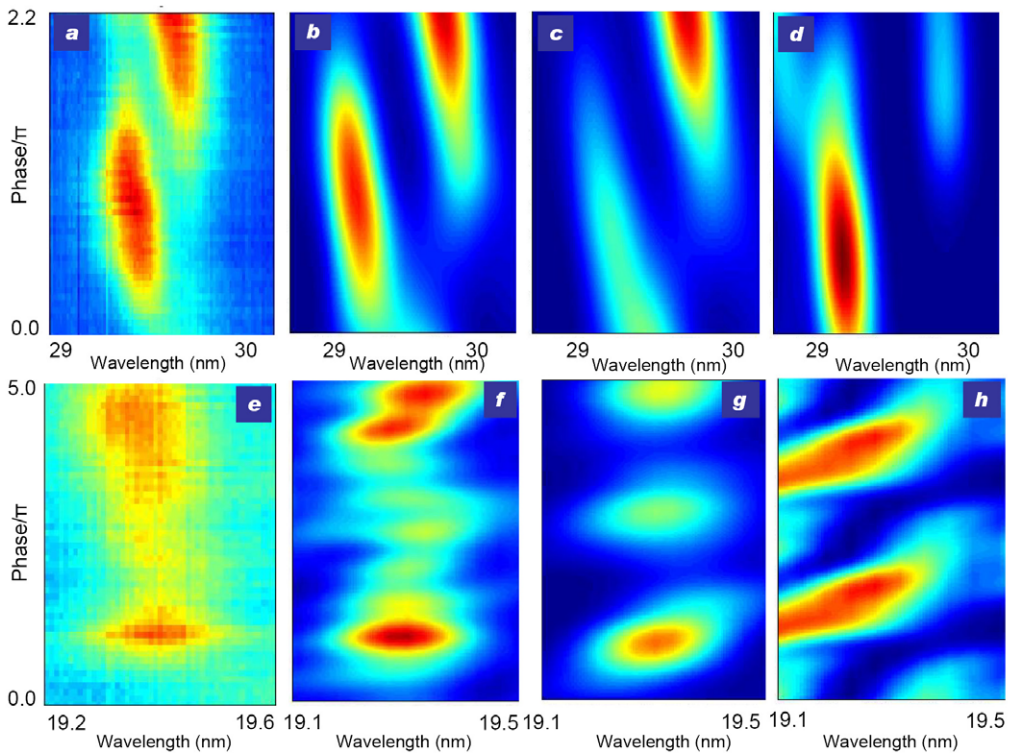

Figure 6. Comparison of the experimental results with 3D simulations. Comparison of the simulated hydrogen pressure scan for the (b) 27th and (f) 41st harmonic to the corresponding experimentally obtained spectra in (a, e). The y-axis shows the relative phase advance (normalized to π) due to the hydrogen matching jets. The agreement between experimental and simulated spectra is excellent. The effects of the hydrogen section on the two trajectory contributions are shown separately for the 27th ((c) short trajectory and (d) long trajectory) and the 41st harmonic ((g) short and (h) long). Note that the color maps of the long trajectory contributions have been enhanced ((d) $\times 100$ compared to (b) and (c); (h) $\times 10$ compared to (f) and (g)).

matching zones. The contributions of the short and long trajectories were accounted for by calculating the complex spectrum for both all short and all long trajectories for the entire pulse and medium length. The matching hydrogen zones were taken into account by treating them as a purely dispersive medium where the plasma dispersion is the dominant phase term. This additional phase was added to the phase of the spectrum of the first jet. This spectrum was then added to that of the second jet, which was calculated separately. Note that the code calculates an electric field $E = E(t, z, \rho)$ with t being the time, z the longitudinal coordinate in the generation volume and ρ the radial coordinate. The third dimension is included assuming axial symmetry, which is very well fulfilled in our experiment. Figures 6(a)–(e) show the radially integrated experimental data with respect to the variation in phase due to hydrogen for the 27th (41st) harmonic already shown in figure 5. The simulated spectra in figures 6(b)–(f) show excellent agreement with the experimental data in terms of the dependence of the spectrum on the phase introduced by the hydrogen matching jet. As mentioned before, our simulation

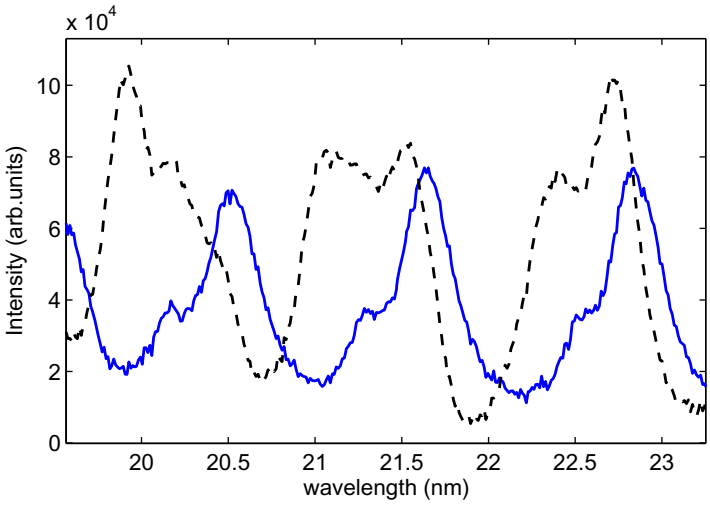

Figure 7. Quantum path control for four sources. With a multi-jet configuration consisting of four source and three matching jets the relative weight of quantum paths is also controllable. Comparing the orders 35–39 at 100 mbar (blue solid) and 1.9 bar (black dashed), hydrogen backing pressure reveals the order-dependent control of the relative weight of the short and long trajectory contributions. The argon backing pressure was 2 bar.

code allows the contribution of the short and long trajectories to be evaluated separately, and figures 6(c)–(g) show the short-trajectory contribution to the 27th (41st harmonic), whereas figures 6(d)–(h) show the long-trajectory contribution. The periodic modulations expected for QPM are now clearly visible for each trajectory as the phase between the HHG sources is varied. The path-dependent intrinsic phase ϕ^j_{QP} leads to a difference in the tuning effect of the passive medium hydrogen for the long and the short trajectory. Thus, strong suppression of the unwanted quantum path can be achieved by setting the relative phase between individual jets such that only the desired trajectory contribution is allowed to build up coherently over many QPM periods. As expected, the matching phase introduced by the hydrogen gas is greater for higher harmonic orders (see equation (1)) leading to a shorter coherence length.

The excellent agreement of the 3D simulations with the measurement demonstrates that the interference between short and long trajectories can be controlled effectively by inserting phase matching zones consisting of fully ionized hydrogen leading to high flexibility of quantum path choice. For FEL seeding, the QPI tuneability allows substantial control over the FEL pulse characteristics in terms of pulse shape and spectral properties by achieving full spatial and spectral coherence in a single harmonic by selecting the short quantum path. Clearly the long trajectory contribution can also be phase matched on axis, adding additional flexibility to the range of wavelengths than can be produced efficiently. This flexibility is of particular interest for increasing the tuneability of the FEL wavelength [14]—albeit potentially at the cost of reduced coherence as discussed above.

To test the ability of quantum path control also for a multi-jet with more than two sources, a further measurement has been carried out with an array consisting of four source and three matching jets. The energy was slightly reduced compared to the previous measurement, whereas all other parameters stayed the same. Figure 7 shows harmonic order 35–39 with 100 mbar

and 1.9 bar hydrogen matching pressure at a constant argon pressure of 2 bar. Similarly to the two-source array, one can clearly see spectral splitting due to quantum path interference, which leads to the easy observation of quantum path-dependent phase matching. For the lower backing pressure of 100 mbar the shorter trajectory is preferentially selected for all three harmonic orders shown. Since the absolute variation of the phase ϕ_q with harmonic order is 19 times larger at the higher pressure, the relative weight of the different spectral contributions changes with order number such that for the 35th (39th) harmonic the short (long) trajectory contribution is dominant, whereas for the 37th harmonic the contributions are of equal strength.

4. Conclusion and outlook

We have shown, for the first time for a multi-jet HHG configuration, coherent control of the two main quantum paths by controlling the relative phase of the sources with matching zones consisting of fully ionized hydrogen gas inserted between the HHG zones. This result is fully supported by 3D simulations which reveal quantum path interference as the origin of the complicated spectral shape. The novel dual-gas QPM scheme allows not only for coherence control, but in principle also for a significant enhancement of the harmonic yield following the scaling law $I_q \propto (N_{\mathrm{QPM}})^2$ with the QPM period N_{QPM}. This combination makes it highly attractive for various applications especially in a wavelength regime where short and long trajectories can be phase matched on axis, which makes an adequate coherence control necessary.

In principle, our scheme will extend to almost any medium as long as the ionization potential of the HHG medium exceeds that of atomic hydrogen and the absorption length is always larger than the actual medium length. Therefore, it will also be possible to exploit high-ionization-potential media offered by ion species while controlling the phase-matching conditions at the same time. Furthermore, we would like to emphasize that our method is in principle also applicable to capillary waveguides, both with and without a discharge, which makes absorption limited HHG using this method applicable to smaller-scale laser systems.

The control mechanism is not limited to any specific number of nozzles and the same behavior as for two sources has also been shown for four sources interspersed with three matching zones. QPM with a dual-gas multi-jet array forms a major step towards the next generation of applications that require highly coherent XUV sources with high repetition rates.

Acknowledgments

The quantum path experiment was performed at the facilities of the Centre of Plasma Physics and Lasers (CPPL), TEI of Crete (www.cppl.teicrete.gr). We are grateful for the outstanding expertise in engineering of Josef Gonschior (DESY Hamburg) who has technically designed the targets and its support. We thank Karl Schmid (MPQ Garching) for discussions concerning the supersonic micro-nozzles. The nozzles were manufactured by CNC Erodiertechnik Burger GmbH. We acknowledge the valuable technical support of Spyros Brezas at CPPL/TEI of Crete. Special thanks are due to Armin Azima (University of Hamburg) for the use of his laser system to measure the gas density forming the basis for the simulation. AW acknowledges financial support from Graduiertenkolleg 1355 of the University of Hamburg.

References

[1] McPherson A *et al* 1987 Studies of multiphoton production of vacuum-ultraviolet radiation in the rare gases *J. Opt. Soc. Am.* B **4** 595

[2] Li X F, L'Huillier A, Ferray M, Lompre L A and Mainfray G 1989 Multiple-harmonic generation in rare gases at high laser intensity *Phys. Rev.* A **39** 5751

[3] Sandberg R L *et al* 2007 Lensless diffractive imaging using tabletop coherent high-harmonic soft-x-ray beams *Phys. Rev. Lett.* **99** 098103

[4] Gagnon E, Ranitovic P, Tong X-M, Cocke C L, Murnane M M, Kapteyn H C and Sandhu A S 2007 Soft x-ray-driven femtosecond molecular dynamics *Science* **317** 1374–8

[5] Haarlammert T and Zacharias H 2009 Application of high harmonic radiation in surface science *Curr. Opin. Solid State Mater. Sci.* **13** 13–27

[6] Siemens M E, Li Q, Murnane M M, Kapteyn H C, Yang R, Anderson E H and Nelson K A 2009 High frequency surface acoustic wave propagation in nanostructures characterized by coherent extreme ultraviolet beams *Appl. Phys. Lett.* **94** 093103

[7] Lambert G *et al* 2008 Injection of harmonics generated in gas in a free-electron laser providing intense and coherent extreme-ultraviolet light *Nature Phys.* **4** 296–300

[8] Corkum P B 1993 Plasma perspective on strong field multiphoton ionization *Phys. Rev. Lett.* **71** 1994

[9] Lewenstein M, Balcou P, Ivanov M Y, L'Huillier A and Corkum P B 1994 Theory of high-harmonic generation by low-frequency laser fields *Phys. Rev.* A **49** 2117

[10] Kim C M and Nam C H 2006 Selection of an electron path of high-order harmonic generation in a two-color femtosecond laser field *J. Phys. B: At. Mol. Opt. Phys.* **39** 3199

[11] Auguste T, Salire P, Wyatt A S, Monmayrant A, Walmsley I A and Cormier E 2009 Theoretical and experimental analysis of quantum path interference in high-order harmonic generation *Phys. Rev.* A **80** 033817

[12] Le Detroff L, Saliere P and Carr B 1998 Beam-quality measurement of a focused high-order harmonic beam *Opt. Lett.* **23** 1544

[13] Mairesse Y *et al* 2004 Optimization of attosecond pulse generation *Phys. Rev. Lett.* **93** 163901

[14] He X *et al* 2009 Spatial and spectral properties of the high-order harmonic emission in argon for seeding applications *Phys. Rev.* A **79** 063829

[15] Auguste T, Carr B and Salire P 2007 Quasi-phase-matching of high-order harmonics using a modulated atomic density *Phys. Rev.* A **76** 011802

[16] Paul A, Bartels R A, Tobey R, Green H, Weiman S, Christov I P, Murnane M M, Kapteyn H C and Backus S 2003 Quasi-phase-matched generation of coherent extreme ultraviolet light *Nature* **42** 51–4

[17] Seres J, Yakovlev V S, Seres E, Streli Ch, Wobrauschek P, Spielmann Ch and Krausz F 2007 Coherent superposition of laser-driven soft-X-ray harmonics from successive sources *Nature Phys.* **3** 878–83

[18] Krausz F and Ivanov M 2009 Attosecond physics *Rev. Mod. Phys.* **81** 163–234

[19] Zhang X, Lytle A L, Popmintchev T, Zhou X, Kapteyn H C, Murnane M M and Cohen O 2007 Quasi-phase-matching and quantum-path control of high-harmonic generation using counterpropagating light *Nature Phys.* **3** 270–5

[20] Faatz B *et al* 2010 FLASH II: perspectives and challenges *Nucl. Instrum. Methods Phys. Res.* A **635** 2–5

[21] Christov I P, Kapteyn H C and Murnane M M 1998 Dispersion-controlled hollow core fiber for phase matched harmonic generation *Opt. Express* **3** 360

[22] Zepf M, Dromey B, Landreman M, Foster P and Hooker S M 2007 Bright quasi-phase-matched soft-x-ray harmonic radiation from argon ions *Phys. Rev. Lett.* **99** 143901

[23] Dromey B, Zepf M, Landreman M and Hooker S M 2007 Quasi-phase-matching of harmonic generation via multimode beating in waveguides *Opt. Express* **15** 7894–900

[24] Lytle A L, Zhang X, Arpin P, Cohen O, Murnane M M and Kapteyn H C 2008 Quasi-phase matching of high-order harmonic generation at high photon energies using counterpropagating pulses *Opt. Lett.* **33** 174–6

[25] Corkum P B, Burnett N H and Ivanov M Y 1994 Subfemtosecond pulses *Opt. Lett.* **19** 1870
[26] Shkolnikov P L, Lago A and Kaplan A E 1994 Optimal quasi-phase-matching for high-order harmonic generation in gases and plasma *Phys. Rev.* A **50** R4461
[27] Pirri A, Corsi C and Bellini M 2008 Enhancing the yield of high-order harmonics with an array of gas jet *Phys. Rev.* A **78** 011801
[28] Gaudiosi D M, Reagan B, Popmintchev T, Grisham M, Berrill M, Cohen O, Walker B C, Murnane M M, Kapteyn H C and Rocca J J 2006 High-order harmonic generation from ions in a capillary discharge *Phys. Rev. Lett.* **96** 203001
[29] Hooker C J *et al* 2006 The Astra Gemini project—a dual beam petawatt Ti:Sapphire laser system *J. Physique* IV **133** 673–7
[30] Tavella F *et al* 2010 Fiber-amplifier pumped high average power few-cycle pulse non-collinear OPCPA *Opt. Express* **18** 4689–94
[31] Rotthardt J *et al* 2010 High average and peak power few-cycle laser pulses delivered by fiber pumped OPCPA system *Opt. Express* **18** 12719–26
[32] Geissler M, Tempea G and Brabec T 2000 Phase-matched high-order harmonic generation in the nonadiabatic limit *Phys. Rev.* A **62** 033817
[33] Tosa V, Yakovlev V S and Krausz F 2008 Generation of tunable isolated attosecond pulses in multi-jet systems *New J. Phys.* **10** 025016
[34] Popmintchev T *et al* 2011 Bright coherent attosecond-to-zeptosecond kiloelectronvolt x-ray supercontinua *Proc. CLEO 2011* (*Baltimore*) PDPC12
[35] Willner A *et al* 2011 Coherent control of high-harmonic generation via dual-gas multijet arrays *Phys. Rev. Lett.* **107** 175002
[36] Yu Q-Z, Li Y-T, Zhang J, Zheng J, Li H-M, Peng X-Y and Li K 2004 Characterization of density profile of cylindrical pulsed gas jets *Chin. Phys. Lett.* **21** 874–6
[37] Kim J-H and Nam Ch H 2002 Plasma-induced frequency chirp of intense femtosecond lasers and its role in shaping high-order harmonic spectral lines *Phys. Rev.* A **65** 033801
[38] Lewenstein M, Balcou Ph, Ivanov M Yu, L'Huillier A and Corkum P B 1994 Theory of high harmonic generation by low frequency laser field *Phys. Rev.* A **49** 2117–32
[39] Ivanov M Yu, Brabec T and Burnett N 1996 Coulomb corrections and polarization effects in high field high harmonic emission *Phys. Rev.* A **54** 742–5
[40] Milosevic N, Scrinzi A and Brabec T 2002 Numerical characterization of high harmonic attosecond pulses *Phys. Rev. Lett.* **88** 093905
[41] Yakovlev V S, Ivanov M and Krausz F 2007 Enhanced phase-matching for generation of soft x-ray harmonics and attosecond pulses in atomic gases *Opt. Express* **15** 15351–64
[42] Cerullo G *et al* 2000 Nonadiabatic three-dimensional model of high-order harmonic generation in the few-optical-cycle regime *Phys. Rev.* A **61** 063801